

1
2
3 **Rapid isolation and profiling of a diverse panel of human monoclonal antibodies targeting**
4 **the SARS-CoV-2 spike protein**
5

6 **AUTHORS:** Seth J. Zost^{1*}, Pavlo Gilchuk^{1*}, Rita E. Chen^{2,9}, James Brett Case³, Joseph X.
7 Reidy¹, Andrew Trivette¹, Rachel S. Nargi¹, Rachel E. Sutton¹, Naveenchandra
8 Suryadevara¹, Elaine C. Chen³, Elad Binshtein¹, Swathi Shrihari⁹, Mario Ostrowski⁴,
9 Helen Y. Chu⁵, Jonathan E. Didier⁶, Keith W. MacRenaris⁶, Taylor Jones¹, Samuel Day¹,
10 Luke Myers¹, F. Eun-Hyung Lee⁷, Doan C. Nguyen⁷, Ignacio Sanz⁷, David R. Martinez⁸,
11 Ralph S. Baric⁸, Larissa B. Thackray⁹, Michael S. Diamond^{2,9,10,11}, Robert H. Carnahan^{1,12**},
12 James E. Crowe, Jr.^{1,3,12**}

13
14 **Affiliations:**

15 ¹Vanderbilt Vaccine Center, Vanderbilt University Medical Center, Nashville, TN, 37232,
16 USA

17 ²Department of Pathology & Immunology, Washington University School of Medicine,
18 St. Louis, MO, 63110, USA

19 ³Department of Pathology, Microbiology, and Immunology, Vanderbilt University Medical
20 Center, Nashville, TN, 37232, USA

21 ⁴Department of Medicine, University of Toronto, Toronto, ON, Canada

22 ⁵Division of Allergy and Infectious Diseases, University of Washington, Seattle 98109, USA

23 ⁶Berkeley Lights, Inc., Emeryville, CA, 94608, USA

24 ⁷Department of Medicine, Emory University, Atlanta, GA, 30322 USA

25 ⁸ Department of Epidemiology, University of North Carolina at Chapel Hill, Chapel Hill,
26 NC, 27599, USA

27 ⁹Department of Medicine, Washington University School of Medicine, St. Louis, 63110,
28 MO, USA

29 ¹⁰Department of Molecular Microbiology, Washington University School of Medicine,
30 St. Louis, MO, 63110, USA

31 ¹¹Andrew M. and Jane M. Bursky Center for Human Immunology and Immunotherapy
32 Programs, Washington University School of Medicine, St. Louis, MO, 63110, USA

33 ¹²Department of Pediatrics, Vanderbilt University Medical Center, Nashville, TN, 37232,
34 USA

35

36 **Contact information:**

37 **James E. Crowe, Jr., M.D. [LEAD CONTACT]**

38 Departments of Pediatrics, Pathology, Microbiology, and Immunology, and the
39 Vanderbilt Vaccine Center

40 **Mail:**

41 Vanderbilt Vaccine Center

42 11475 Medical Research Building IV

43 2213 Garland Avenue

44 Nashville, TN 37232-0417, USA

45 **Telephone** (615) 343-8064

46 **Email** james.crowe@vumc.org

47 **Additional Title Page Footnotes**

48 * These authors contributed equally

49 **Corresponding authors

50

51

52 **Keywords:** Coronavirus; SARS-CoV-2; SARS-CoV; COVID-19; Antibodies, Monoclonal;

53 Human; Adaptive Immunity.

54 **Antibodies are a principal determinant of immunity for most RNA viruses and have**
55 **promise to reduce infection or disease during major epidemics. The novel**
56 **coronavirus SARS-CoV-2 has caused a global pandemic with millions of infections**
57 **and hundreds of thousands of deaths to date^{1,2}. In response, we used a rapid**
58 **antibody discovery platform to isolate hundreds of human monoclonal antibodies**
59 **(mAbs) against the SARS-CoV-2 spike (S) protein. We stratify these mAbs into five**
60 **major classes based on their reactivity to subdomains of S protein as well as their**
61 **cross-reactivity to SARS-CoV. Many of these mAbs inhibit infection of authentic**
62 **SARS-CoV-2 virus, with most neutralizing mAbs recognizing the receptor-binding**
63 **domain (RBD) of S. This work defines sites of vulnerability on SARS-CoV-2 S and**
64 **demonstrates the speed and robustness of new antibody discovery methodologies.**

65
66 Human mAbs to the viral surface spike (S) glycoprotein mediate immunity to other
67 betacoronaviruses including SARS-CoV³⁻⁷ and Middle East respiratory syndrome
68 (MERS)⁸⁻¹⁷. Because of this, we and others have hypothesized that human mAbs may
69 have promise for use in prophylaxis, post-exposure prophylaxis, or treatment of SARS-
70 CoV-2 infection¹⁸. MAbs can neutralize betacoronaviruses by several mechanisms
71 including blocking of attachment of the S protein RBD to a receptor on host cells (which
72 for SARS-CoV and SARS-CoV-2¹ is angiotensin-converting enzyme 2 [ACE2])¹². We
73 hypothesized that the SARS-CoV-2 S protein would induce diverse human neutralizing
74 antibodies following natural infection. While antibody discovery usually takes months
75 to years, there is an urgent need to both characterize the human immune response to
76 SARS-CoV-2 infection and to develop potential medical countermeasures. Using Zika
77 virus as a simulated pandemic pathogen and leveraging recent technological advances
78 in synthetic genomics and single-cell sequencing, we recently isolated hundreds of

79 human mAbs from a single B cell suspension and tested them *in vitro* for neutralization
80 and for protection in small animals and nonhuman primates, all within 78 days¹⁹. Using
81 similar methodologies and further efficiency improvements, we sought to obtain
82 human mAbs rapidly for SARS-CoV-2 from the B cells of some of the first human
83 subjects identified with infection in North America. We used an approach similar to
84 that in our previous technical demonstration with Zika, however, for the SARS-CoV-2
85 discovery effort we report here we used several different workflows in parallel (**Figure**
86 **1, Table S2**), which we completed in an expedited time frame (**Figure 1**).

87
88 We first developed or obtained antigens and recombinant proteins necessary for
89 identifying and isolating antigen-reactive B cells. We synthesized a cDNA encoding a
90 stabilized trimeric prefusion ectodomain of S protein (S2P_{ecto})²⁰, expressed the protein in
91 293F cells, and verified the presence of the prefusion conformation by electron
92 microscopy (**Figure S1**). We also synthesized and expressed the S protein receptor
93 binding domain (S_{RBD}) and obtained recombinant S protein N terminal domain (S_{NTD})
94 that had been prepared by other academic or commercial sources. Using these tools, we
95 designed a mAb discovery approach focused on identifying naturally occurring human
96 mAbs specific for S.

97
98 We obtained blood samples from four subjects infected in China who were among the
99 earliest identified SARS-CoV-2-infected patients in North America (**Table S1**). These
100 subjects had a history of recent laboratory-confirmed SARS-CoV-2 infection acquired in
101 Wuhan or Beijing, China. The samples were obtained 35 days (subject 1; the case
102 identified in the U.S.²¹), 36 days (subject 2), or 50 days (subjects 3 and 4) after the onset
103 of symptoms. We tested plasma or serum specimens from the four subjects infected

104 with SARS-CoV-2, or from a healthy donor (subject 5) as control. Serum/plasma
105 antibody ELISA binding assays using S2P_{ecto}, S_{RBD}, or S_{NTD} protein from SARS-CoV-2 or
106 S2P_{ecto} protein from SARS-CoV revealed that the previously infected subjects had
107 circulating antibodies that recognized each of the proteins tested, with highest reactivity
108 against SARS-CoV-2 S2P_{ecto} and S_{RBD} proteins (**Figure 2a**). Each of the immune subjects
109 also had circulating antibodies that bound to SARS-CoV S2P_{ecto}. The healthy donor
110 serum antibodies did not react with any of the antigens. B cells were enriched from
111 PBMCs by negative selection using antibody-coated magnetic beads and stained with
112 phenotyping antibodies specific for CD19, IgD, and IgM. Analytical flow cytometry was
113 performed to assess the frequency of antigen-specific memory B cells for each donor.
114 We identified class-switched memory B cells by gating for an IgD⁻/IgM⁻/CD19⁺
115 population (**Figure 2b**). From this memory B cell population, we identified antigen-
116 reactive cells using biotinylated recombinant S2P_{ecto} protein or biotinylated RBD fused
117 to mouse Fc (RBD-mFc). Subjects 1 and 2 had very low frequencies of antigen-specific
118 memory B cells that were not greater than two-fold above the background staining
119 frequency in a non-immune sample (subject 6) (**Figure 2c**). In contrast to subjects 1 and
120 2, subjects 3 and 4 were 2 weeks later in convalescence and exhibited 0.62 or 1.22 % of
121 class-switched B cells that reacted with antigen (**Figure 2c**). Subjects 3 and 4 also
122 exhibited high titers in a serum antibody focus reduction neutralization test (FRNT)
123 with an authentic SARS-CoV-2 strain (WA/1/2020) (**Figure 2d**). Therefore, we focused
124 subsequent efforts on sorting B cells from the specimens of subjects 3 and 4, which were
125 pooled for efficiency. The pooled memory B cell suspension had frequencies for S2P_{ecto}
126 or RBD-mFc that were 0.81 or 0.19% of the IgD⁻/IgM⁻/CD19⁺ population, respectively
127 (**Figure 2e**). The bulk sorted S2P_{ecto}- or RBD-mFc-specific B cells were stimulated on a
128 feeder layer with CD40L, IL-21 and BAFF²², and the secreted antibodies in the resulting

129 cell culture supernatants exhibited neutralizing activity against the WA1/2020 strain
130 (**Figure 2f**). After 7 days in culture, these activated B cells were removed from the
131 feeder layers. Roughly half of these B cells were single-cell sequenced and antibody
132 genes were synthesized as previously described¹⁹. The remaining cells were loaded onto
133 a Berkeley Lights Beacon optofluidic instrument in a novel plasma cell survival
134 medium, and antigen reactivity of secreted antibody from individual B cells was
135 measured for thousands of cells (**Figure S2**). Antigen-reactive B cells were exported
136 from the instrument and the heavy and light chain genes from single B cells were
137 sequenced and cloned into immunoglobulin expression vectors.

138
139 Using the parallel workflows, we isolated 386 recombinant SARS-CoV-2-reactive
140 human mAbs that expressed sufficiently well as recombinant IgG to characterize the
141 activity of the mAb. The recombinant mAbs were tested for binding in ELISA to
142 recombinant monomeric S_{RBD} or S_{NTD} of SARS-CoV-2 or trimeric $S2P_{\text{ecto}}$ proteins of
143 SARS-CoV-2 or SARS-CoV (**Figure 3a**) and in a cell-impedance based SARS-CoV-2
144 neutralization assay with WA1/2020 strain SARS-CoV-2 in Vero-furin cells (**Figure S3**).
145 The ELISA and neutralization screening assays revealed that the antibodies could be
146 grouped into five binding patterns based on domain recognition and cross-reactivity
147 (**Figure 3b**). Comparison of binding patterns with full or partial neutralizing activity in
148 a rapid cell-impedance-based SARS-CoV-2 neutralization test (**Figure 3c**) showed
149 clearly that most of the neutralizing antibodies mapped to the RBD, revealing the RBD
150 as the principal site of vulnerability for SARS-CoV-2 neutralization in these subjects. We
151 examined the sequences for the 386 antibodies to assess the diversity of antigen-specific
152 B cell clonotypes discovered. The analysis showed that among the 386 mAbs, 324
153 unique amino sequences were present and 311 unique $V_{\text{H}}\text{-}J_{\text{H}}\text{-}CDRH3\text{-}V_{\text{L}}\text{-}J_{\text{L}}\text{-}CDRL3$

154 clonotypes were represented, with diverse usage of antibody variable genes (**Figure 3d**).
155 The CDR3 amino acid length distributions in the heavy and light chains were typical of
156 human repertoires (**Figure 3e**)²³. The high relatedness of sequences to the inferred
157 unmutated ancestor antibody genes observed for this panel of antibodies (**Figure 3f**)
158 contrasts with the much higher frequencies seen in B cell recall responses against
159 common human pathogens like influenza²⁴. These data suggest that the SARS-CoV-2
160 antibodies likely were induced during the primary response to SARS-CoV-2 infection
161 and not by a recall response to a distantly related seasonal coronavirus. To validate the
162 neutralizing activity measured in the cell-impedance-based neutralization test, we also
163 confirmed neutralization for representative mAbs in a quantitative FRNT assay for
164 SARS-CoV-2 (**Figure 3g**) or a neutralization assay with a SARS-CoV luciferase reporter
165 virus (**Figure 3h**). Together, these results confirmed that mAbs recognizing multiple
166 epitopes on S were able to neutralize SARS-CoV-2 and cross-react with SARS-CoV, with
167 most neutralizing mAbs specific for the RBD of S.

168
169 Here, we coupled single-B-cell RNAseq methods with high-throughput IgG micro-
170 expression and real-time neutralization assays to isolate and profile a large number of
171 neutralizing antibodies in a period of only weeks after sample acquisition. As we show,
172 recent advances in single-cell sequencing and gene synthesis have enabled antibody
173 discovery at unprecedented scale and speed. In our particular example, sequences of
174 confirmed neutralizing antibodies were transferred to downstream manufacturing
175 partners only 18 days after antigen-specific cell sorting. However, given the need for
176 affinity maturation and the development of a mature B cell response there are limits on
177 the timeline from infection to isolation of potent neutralizing antibodies with
178 therapeutic promise. It has been previously shown for Ebola virus infection that

179 potentially neutralizing antibodies are not easily isolated from memory B cells until later
180 timepoints in the first year after infection^{25,26}. It is likely that our success in isolating
181 neutralizing antibodies from subjects 3 and 4 here at 50 days after onset, but not from
182 subjects 1 and 2 at 35 or 36 days after onset, reflected additional maturation of the
183 memory B cell response that occurred in the additional two weeks convalescence.
184 Overall, our work illustrates the promise of coupling recent technological advances for
185 antibody discovery and defines the RBD of SARS-CoV-2 S as a major site of
186 vulnerability for vaccine design and therapeutic antibody development. The most
187 potent neutralizing human mAbs isolated here also could serve as candidate biologics
188 to prevent or treat SARS-CoV-2 infection.

189
190 **Acknowledgements.** We thank Merissa Mayo and Norma Suazo Galeano for coordination of
191 human subjects studies, David O'Connor, Nasia Safdar, Geoff Baird, Jay Shendure and
192 Samira Mubareka for helpful advice on human subjects, Angela Jones and the staff of the
193 Vanderbilt VANTAGE core laboratory for expedited sequencing, Ross Trosseth for assistance
194 with data management and analysis, Robin Bombardi and Cinque Soto for technical
195 consultation on genomics approaches, Arthur Kim for production of a recombinant form of
196 the mAb CR3022, Chris Swearingen and the staff of Fedex Express Specialty Services for
197 expedited transport services, Vincent Pai and Keith Breinlinger of Berkeley Lights, Inc., and
198 Kevin Louder and scientists at Twist Bioscience, Brian Fritz at 10x Genomics, and
199 representatives at ACEA Biosciences for providing resources, outstanding expedited services
200 and expert applications support. We thank Andrew Ward, Sandhya Bangaru and Nicole-
201 Kallewaard-Lelay for protein reagents. This study was supported by Defense Advanced
202 Research Projects Agency (DARPA) grant HR0011-18-2-0001, NIH contracts 75N93019C00074
203 and 75N93019C00062 and the Dolly Parton COVID-19 Research Fund at Vanderbilt. This

204 work was supported by NIH grant 1S10RR028106-01A1 for the Next Generation Nucleic Acid
205 Sequencer, housed in Vanderbilt Technologies for Advanced Genomics (VANTAGE) and
206 supported by the National Center for Research Resources, Grant UL1 RR024975-01, and is
207 now at the National Center for Advancing Translational Sciences, Grant 2 UL1 TR000445-06.
208 S.J.Z. was supported by NIH T32 AI095202. J.B.C. is supported by a Helen Hay Whitney
209 Foundation postdoctoral fellowship D.R.M. was supported by NIH T32 AI007151 and a
210 Burroughs Wellcome Fund Postdoctoral Enrichment Program Award. J.E.C. is the recipient of
211 the 2019 Future Insight Prize from Merck KGaA, Darmstadt Germany, which supported this
212 research with a research grant. The content is solely the responsibility of the authors and does
213 not necessarily represent the official views of the U.S. government or the other sponsors.

214

215 **Author contributions.** Conceived of the project: S.J.Z., P.G., R.H.C., L.B.T., M.S.D.,
216 J.E.C.; Obtained funding: J.E.C. and M.S.D. Obtained human samples: M.O., H.Y.C.,
217 J.E.C.; Performed laboratory experiments: S.J.Z., P.G., R.E.C., J.X.R., A.T., R.S.N., R.E.S.,
218 N.S., E.B., J.E.D., K.W.M., S.S., D.R.M; Performed computational work: E.C.C., T.J., S.D.,
219 L.M.; Supervised research: M.S.D., L.B.T., R.S.B., R.H.C., J.E.C. Provided critical
220 reagents: J.E.D., K.W.M., F.E.-H.L., D.C.N., I.S., R.S.B. Wrote the first draft of the paper:
221 S.J.Z., P.G., R.H.C., J.E.C.; All authors reviewed and approved the final manuscript.

222

223 **Competing interests.** R.S.B. has served as a consultant for Takeda and Sanofi Pasteur on
224 issues related to vaccines. M.S.D. is a consultant for Inbios, Vir Biotechnology, NGM
225 Biopharmaceuticals, Eli Lilly, and on the Scientific Advisory Board of Moderna, and a recipient
226 of unrelated research grants from Moderna and Emergent BioSolutions. H.Y.C. has served as
227 a consultant for Merck and GlaxoSmithKline, research funding from Sanofi Pasteur and
228 research support from Cepheid, Genentech, and Ellume. J.E.C. has served as a consultant for

229 Sanofi and is on the Scientific Advisory Boards of CompuVax and Meissa Vaccines, is a
230 recipient of previous unrelated research grants from Moderna and Sanofi and is Founder of
231 IDBiologics, Inc. Vanderbilt University has applied for patents concerning SARS-CoV-2
232 antibodies that are related to this work. Emory University has applied for a patent concerning
233 the plasmablast survival medium. J.E.D. and K.W.M. are employees of Berkeley Lights, Inc.
234 All other authors declared no competing interests.

235

236 **Data availability.** All relevant data are included with the manuscript.

237 **Figure Legends**

238

239

240 **Figure 1. Workflows and timelines.**

241 **a. Overview of rapid monoclonal antibody discovery workflows.** The overall scheme

242 is shown, representing the seven specific workflows conducted in parallel (specified in

243 **Table S2**). Blood was collected and white blood cells separated, B cells were enriched

244 from PBMCs by negative selection using paramagnetic beads, antigen-specific cells

245 were obtained by flow cytometric sorting, then processed for direct B cell selection and

246 sequencing or *in vitro* expansion/activation. Cultured B cells were loaded on a Beacon

247 instrument (Berkeley Lights) for functional screening (**Figure S2, Movie S1**) or in a

248 Chromium device (10X Genomics) followed by RT-PCR, sequence analysis, cDNA gene

249 synthesis and cloning into an expression vector, and microscale IgG expression in CHO

250 cells by transient transfection. Recombinant IgG was tested by ELISA for binding to

251 determine antigen reactivity and by a cell impedance-based neutralization test

252 (xCelligence; ACEA) (**Figure S3**) with live virus in a BSL3 laboratory for functional

253 characterization.

254

255 **Figure 2. Characterization of SARS-CoV-2 immune donor samples.**

256 **a. Serum or plasma antibody reactivity** for the four SARS-CoV-2 immune subjects or

257 one non-immune control, in ELISA using SARS-CoV-2 S2P_{ecto}, S_{RBD}, S_{NTD}, SARS-CoV

258 S2P_{ecto} or PBS.

259 **b. Gating for memory B cells** in total B cells enriched by negative selection using

260 magnetic beads for subject 4; Cells were stained with anti-CD19 antibody conjugated to

261 allophycocyanin (APC) and anti-IgM and anti-IgD antibodies conjugated to fluorescein

262 isothiocyanate (FITC).

263 **c. Analytical flow cytometric analysis of B cells** for subjects 1 to 4, compared to a
264 healthy subject (subject 6). Plots show CD19⁺IgD⁻IgM⁻ population using gating strategy
265 as in **b**. Cells labeled with biotinylated S2P_{ecto} or RBD-mFc antigens were detected using
266 phycoerythrin (PE)-conjugated streptavidin.

267 **d. Plasma or serum neutralizing activity** against the WA1/2020 strain SARS-CoV-2 for
268 subjects 1 to 4 or a healthy donor (subject 6). % neutralization is reported.

269 **e. FACS isolation of S2P_{ecto} or RBD-mFc-reactive B cells** from pooled B cells of subject 3
270 and 4. Plots show CD19⁺IgD⁻IgM⁻ population using gating strategy as in **b**, and antigen-
271 reactive B cells were identified as in **c**.

272 **f. Lymphoblastoid cell line (LCL) supernatant neutralization.** Neutralization of the
273 WA1/2020 strain SARS-CoV-2 by supernatant collected from cell cultures of S2P_{ecto}- or
274 RBD-mFc-sorted memory B cells that had been stimulated in bulk *in vitro* on feeder
275 layers expressing CD40L and secreting IL-21 and BAFF. The supernatants were tested
276 in a ten-point dilution series in the FRNT, and % neutralization is reported. Values
277 shown are the mean ± SD of technical duplicates.

278

279 **Figure 3. Reactivity and functional activity of 386 human mAbs.**

280 **a. Structures of SARS-CoV-2 spike antigen.** Top panel: S protein monomer of SARS-
281 CoV-2 highlighting RBD (blue) and NTD (red) subdomains that were expressed as
282 recombinant proteins. The ACE2 binding site on RBD is shown in orange. Known
283 glycans are shown as light grey spheres. (PDB 6VYB) Middle panel: the structure of
284 trimeric SARS-CoV-2 spike with one RBD in the “head up” conformation. Bottom panel:
285 structure (PDB 6M0J) of SARS-CoV-2 RBD (blue) and ACE2 (pink) highlighting
286 differences between RBDs of SARS-CoV-2 and SARS-CoV (cyan).

287 **b. MAbs binding to each of four S proteins or subdomains.** The figure shows a
288 heatmap for binding of 386 mAbs expressed recombinantly, representing optical
289 density (O.D.) values collected at 450 nm for each antigen (range 0.035 to 4.5). White
290 indicates lack of detectable binding, while blue indicates binding, with darker blue
291 indicating higher O.D. values.

292 **c. Screening test for neutralizing activity.** Each mAb was tested in a cell-impedance
293 based neutralization test (**Figure S3**) using Vero-furin cells and live WA1/2020 strain
294 SARS-CoV-2 in a BSL3 laboratory. Green indicates full protection of cells (full
295 neutralization), purple indicates partial protection of cells, (partial neutralization), and
296 white indicates neutralizing activity was not detected. Based on both binding and
297 neutralization, we grouped the mAbs into classes. Class I mAbs bind to both S2P_{ecto} and
298 S_{RBD} proteins and are SARS-CoV-2 specific; Class II mAbs also bind to both S2P_{ecto} and
299 S_{RBD} proteins and cross-react with SARS-CoV; Class III mAbs bind to both S2P_{ecto} and
300 S_{NTD} proteins and are mostly SARS-CoV-2 specific; Class IV mAbs bind only to S2P_{ecto}
301 protein and are SARS-CoV-2 specific; Class V mAbs bind only to S2P_{ecto} protein and
302 cross-react with SARS-CoV.

303 **d. Heatmap showing usage of antibody variable gene segments for variable (V) and**
304 **joining (J) genes.** Of the 386 antibodies tested in (b) and (c) above, 324 were found to
305 have unique sequences, and those unique sequences were analyzed for genetic features.
306 The frequency counts are derived from the total number of unique sequences with the
307 corresponding V and J genes. The V/J frequency counts then were transformed into a z-
308 score by first subtracting the average frequency, then normalizing by the standard
309 deviation of each subject. Red denotes more common gene usage, while blue denotes
310 less common gene usage.

311 **e. CDR3 amino acid length distribution.** The CDR3 of each sequence was determined
312 using PyIR software. The amino acid length of each CDR3 was counted. The
313 distribution of CDR3 amino acid lengths for heavy or light chains then was plotted as a
314 histogram and fitted using kernel density estimation for the curves.

315 **f. Divergence from inferred germline gene sequences.** The number of mutations from
316 each inferred unmutated ancestor sequence in the region spanning from antibody
317 framework region 1 to 4 was counted up for each chain. These numbers then were
318 transformed into percent values and plotted as violin plots.

319 **g. Quantitative test for neutralizing activity against SARS-CoV-2 using FRNT.**

320 Representative mAbs that exhibited full neutralizing activity in the screening
321 neutralization test in (c) above using micro-scale expression were prepared in midi-
322 scale as purified IgG and tested in a serial dilution series in the FRNT with live
323 WA1/2020 strain SARS-CoV-2 to demonstrate neutralizing potency of class-
324 representative mAbs. % neutralization of virus infection (relative to control wells with
325 no mAb) at each dilution is shown. Values shown are the mean of two technical
326 replicates, and error bars denote the standard deviation for each point.

327 **h. Quantitative test for neutralizing activity against SARS-CoV using a nano-**

328 **luciferase virus.** A representative purified mAb that exhibited cross-reactive binding to
329 SARS-CoV S2P_{ecto} protein in (b) above and that also exhibited full neutralizing activity
330 in the screening neutralization test in (c) above was tested in a serial dilution series in a
331 neutralization test with a recombinant, reverse-genetics-derived SARS-CoV encoding a
332 nano-luciferase reporter gene, and reduction of luciferase activity was used to calculate
333 % neutralization. Values shown are the mean of two technical replicates, and error bars
334 denote the standard deviation for each point.

335

336 **Supplementary Information**

337

338

339 **Figure S1. Expression and validation of prefusion-stabilized SARS-CoV-2 S2P_{ecto}**

340 **protein.**

341 **a.** Reducing SDS-PAGE gel indicating S2P_{ecto} protein migrating at approximately

342 180KDa.

343 **b. Representative micrograph of negative-stain electron microscopy with S2P_{ecto}**

344 **protein preparation.** Scale bar denotes 100 nm.

345 **c. 2D class-averages of S2P_{ecto} protein in the prefusion conformation.** The size for each

346 box is 128 pixels.

347

348 **Figure S2. Functional assays from single antigen-reactive B cells.**

349 **a. Schematic of detection of antigen-specific antibody.** Biotinylated antigen (dark
350 grey) was coupled to a streptavidin-conjugated polystyrene bead (light grey).

351 Antibodies (blue) are secreted by single B cells loaded into individual NanoPens on the
352 Berkeley Lights Beacon optofluidic device. Antibody binding to antigen was detected
353 with a fluorescent anti-human IgG secondary Ab (black).

354 **b. Left:** Schematic of fluorescing beads in the channel above a pen containing an
355 individual B cell indicates antigen-specific reactivity.

356 **Top right:** False-color still image of positive wells with B cells secreting S2P_{ecto}-
357 reactive antibodies. Reactive antibody diffusing out of a pen is visualized as a plume of
358 fluorescence.

359 **Bottom right:** False-color still image of positive wells with B cells secreting RBD-
360 mFc-reactive antibodies. **c.** Representative images of RBD-mFc reactive clones.

361

362 **Figure S3. Real-time cell analysis assay to screen for neutralization activity.**

363 **a. Representative sensograms for neutralizing mAbs.** Curves for fully neutralizing mAb
364 (green) and partially neutralizing mAb (red) by monitoring of CPE in Vero-furin cells that
365 were inoculated with SARS-CoV-2 and pre-incubated with the respective mAb. Uninfected
366 cells (blue) and infected cells without antibody addition (grey) served as controls for intact
367 monolayer and full CPE, respectively. Data represented single well measurement for each
368 mAb and mean SD values of technical duplicates or quadruplicates for the controls.

369 **b. Example sensograms from individual wells of 384-well E-plate analysis showing rapid**
370 **identification of SARS-CoV-2 neutralizing mAbs.** Neutralization was assessed using
371 micro-scale purified mAbs and each mAb was tested in four 5-fold dilutions as indicated.
372 Plates were measured every 8-12 hours for a total of 72 hrs as in (a).

373

374

375 **Movie S1. Time-lapse imaging of antigen-sorted single B cells secreting S2P_{ecto}-**

376 **reactive antibodies.** A field of view of the optofluidic chip is shown with single B cells
377 at the bottom of NanoPens, as in Figure S1. Antigen-reactive antibody bound to S2P_{ecto}
378 antigen conjugated to streptavidin polystyrene beads loaded into the channel is
379 detected by an anti-IgG secondary antibody. Positive wells are identified by the specific
380 bloom of fluorescence signal, indicating antigen-specific antibody diffusing out of a
381 single pen. The edges of pens are highlighted in green and pen numbers are shown in
382 yellow. For that field of view, there were 96 pens containing B cells, with 53 cells
383 secreting trimer-reactive antibody and 30 cells secreting antibody reactive to RBD. The
384 movie is composed of still images obtained every five minutes over the course of a 30-
385 minute assay.

386 **References**

387

388 1. Zhou, P., *et al.* A pneumonia outbreak associated with a new coronavirus of
389 probable bat origin. *Nature* **579**, 270-273 (2020).

390

391 2. Zhu, N., *et al.* A novel coronavirus from patients with pneumonia in China, 2019.
392 *N Engl J Med* **382**, 727-733 (2020).

393

394 3. Sui, J., *et al.* Potent neutralization of severe acute respiratory syndrome (SARS)
395 coronavirus by a human mAb to S1 protein that blocks receptor association. *Proc*
396 *Natl Acad Sci U S A* **101**, 2536-2541 (2004).

397

398 4. ter Meulen, J., *et al.* Human monoclonal antibody as prophylaxis for SARS
399 coronavirus infection in ferrets. *Lancet* **363**, 2139-2141 (2004).

400

401 5. ter Meulen, J., *et al.* Human monoclonal antibody combination against SARS
402 coronavirus: synergy and coverage of escape mutants. *PLoS Med* **3**, e237 (2006).

403

404 6. Zhu, Z., *et al.* Potent cross-reactive neutralization of SARS coronavirus isolates by
405 human monoclonal antibodies. *Proc Natl Acad Sci U S A* **104**, 12123-12128 (2007).

406

407 7. Rockx, B., *et al.* Structural basis for potent cross-neutralizing human monoclonal
408 antibody protection against lethal human and zoonotic severe acute respiratory
409 syndrome coronavirus challenge. *J Virol* **82**, 3220-3235 (2008).

410

- 411 8. Chen, Z., *et al.* Human neutralizing monoclonal antibody inhibition of Middle East
412 respiratory syndrome coronavirus replication in the common marmoset. *J Infect*
413 *Dis* **215**, 1807-1815 (2017).
414
- 415 9. Choi, J.H., *et al.* Characterization of a human monoclonal antibody generated from
416 a B-cell specific for a prefusion-stabilized spike protein of Middle East respiratory
417 syndrome coronavirus. *PLoS One* **15**, e0232757 (2020).
418
- 419 10. Niu, P., *et al.* Ultrapotent human neutralizing antibody repertoires against Middle
420 East respiratory syndrome coronavirus from a recovered patient. *J Infect Dis* **218**,
421 1249-1260 (2018).
422
- 423 11. Wang, L., *et al.* Importance of neutralizing monoclonal antibodies targeting
424 multiple antigenic sites on the Middle East respiratory syndrome coronavirus
425 spike glycoprotein to avoid neutralization escape. *J Virol* **92**(2018).
426
- 427 12. Wang, N., *et al.* Structural Definition of a Neutralization-Sensitive Epitope on the
428 MERS-CoV S1-NTD. *Cell Rep* **28**, 3395-3405 e3396 (2019).
429
- 430 13. Zhang, S., *et al.* Structural definition of a unique neutralization epitope on the
431 receptor-binding domain of MERS-CoV spike glycoprotein. *Cell Rep* **24**, 441-452
432 (2018).
433

- 434 14. Corti, D., *et al.* Prophylactic and postexposure efficacy of a potent human
435 monoclonal antibody against MERS coronavirus. *Proc Natl Acad Sci U S A* **112**,
436 10473-10478 (2015).
437
- 438 15. Jiang, L., *et al.* Potent neutralization of MERS-CoV by human neutralizing
439 monoclonal antibodies to the viral spike glycoprotein. *Sci Transl Med* **6**, 234ra259
440 (2014).
441
- 442 16. Tang, X.C., *et al.* Identification of human neutralizing antibodies against MERS-
443 CoV and their role in virus adaptive evolution. *Proc Natl Acad Sci U S A* **111**, E2018-
444 2026 (2014).
445
- 446 17. Ying, T., *et al.* Exceptionally potent neutralization of Middle East respiratory
447 syndrome coronavirus by human monoclonal antibodies. *J Virol* **88**, 7796-7805
448 (2014).
449
- 450 18. Jiang, S., Hillyer, C. & Du, L. Neutralizing antibodies against SARS-CoV-2 and
451 other human coronaviruses. *Trends Immunol* **41**, 355-359 (2020).
452
- 453 19. Gilchuk P, B.R., Erasmus JH, Durnel LA, Nargi R, Soto C, Abbink P, Suscovich TJ,
454 Tan Q, Khandhar A, Archer J, Bryan A, Davidson E, Doranz BJ, Fouch ME, Jones
455 T, Larson E, Ertel S, Granger B, Fuerte-Stone J, Roy V, Broge T, Linnekin TC, Linde
456 CH, Gorman MJ, Nkolola J, Galit Alter G, Steven G Reed SG, Daniel H Barouch
457 DH, Michael S Diamond MS, Crowe JE Jr, Neal Hoeven N, Thackray L, Carnahan

- 458 R. Integrated technology platform for accelerated discovery of antiviral antibody
459 therapeutics. . *Nature Medicine* (2020).
460
- 461 20. Wrapp, D., *et al.* Cryo-EM structure of the 2019-nCoV spike in the prefusion
462 conformation. *Science* **367**, 1260-1263 (2020).
463
- 464 21. Holshue, M.L., *et al.* First case of 2019 novel coronavirus in the United States. *N*
465 *Engl J Med* **382**, 929-936 (2020).
466
- 467 22. Gilchuk, P., *et al.* Analysis of a Therapeutic antibody cocktail reveals determinants
468 for cooperative and broad ebolavirus neutralization. *Immunity* **52**, 388-403 e312
469 (2020).
470
- 471 23. Soto, C., *et al.* High frequency of shared clonotypes in human B cell receptor
472 repertoires. *Nature* **566**, 398-402 (2019).
473
- 474 24. Wrammert, J., *et al.* Broadly cross-reactive antibodies dominate the human B cell
475 response against 2009 pandemic H1N1 influenza virus infection. *J Exp Med* **208**,
476 181-193 (2011).
477
- 478 25. Williamson, L.E., *et al.* Early human B cell Rrsponse to Ebola virus in four U.S.
479 survivors of infection. *J Virol* **93**(2019).
480
- 481 26. Davis, C.W., *et al.* Longitudinal analysis of the human B cell response to Ebola
482 virus infection. *Cell* **177**, 1566-1582 e1517 (2019).

**Discovery approach #1:
single-cell sequencing
gene synthesis**

**Discovery approach #2:
single-cell functional assays
sequencing and cloning**

Sorting
(Day 1)

Sorting
(Day 1)

Blood collection
PBMC isolation

B cell enrichment

Antigen-specific sorting

Sequencing
(Day 1-3)

Sequencing
(Day 8-9)

Expansion
(Days 1-8)

Single-cell sequencing
Bioinformatic analysis

in vitro expansion

Synthesis
(Day 10-28)

Single-cell
assays
(Day 9)

Gene synthesis

Single-cell antibody secretion assays
Sequencing and cloning

Expression
(Day 28-32)

Sequencing,
cloning
(Days 9-13)

IgG
expression
vector

Transient transfection

CHO
cells

Expression
(Day 14-17)

Microscale expression

Neutralization
(Day 35)

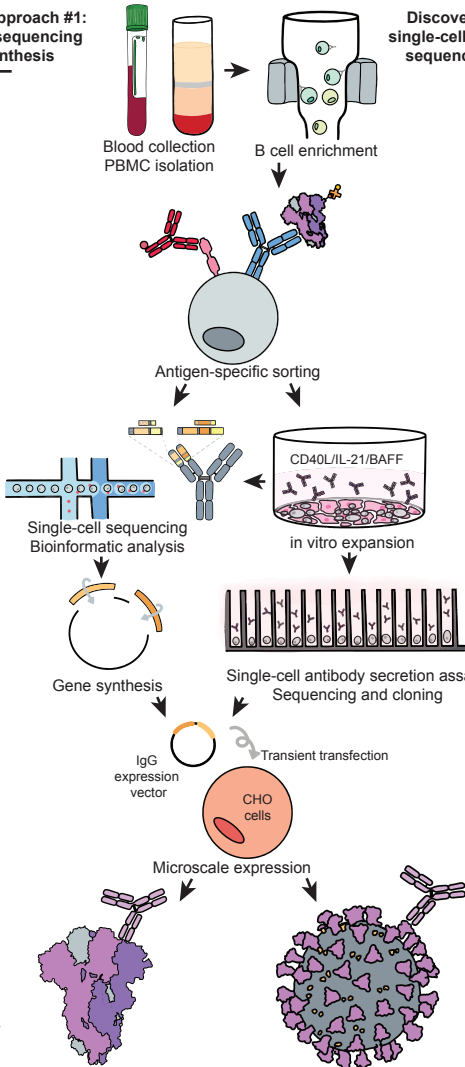
Neutralization
(Day 18)

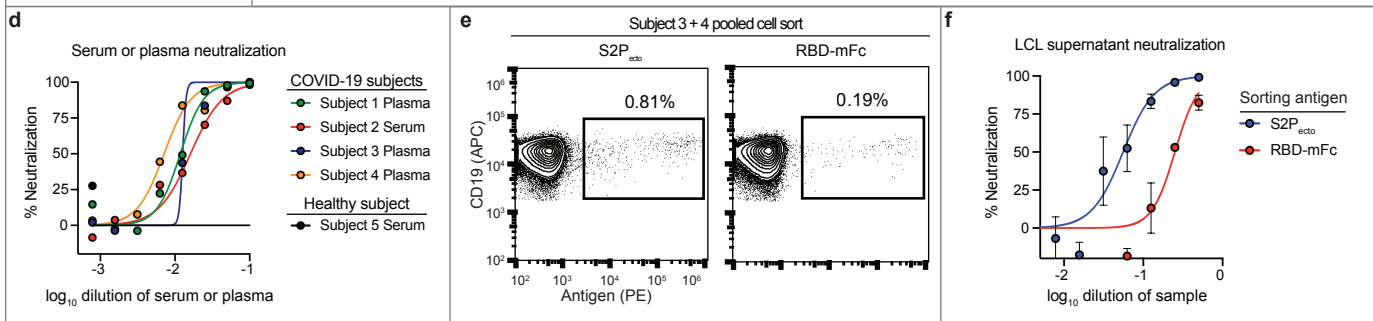
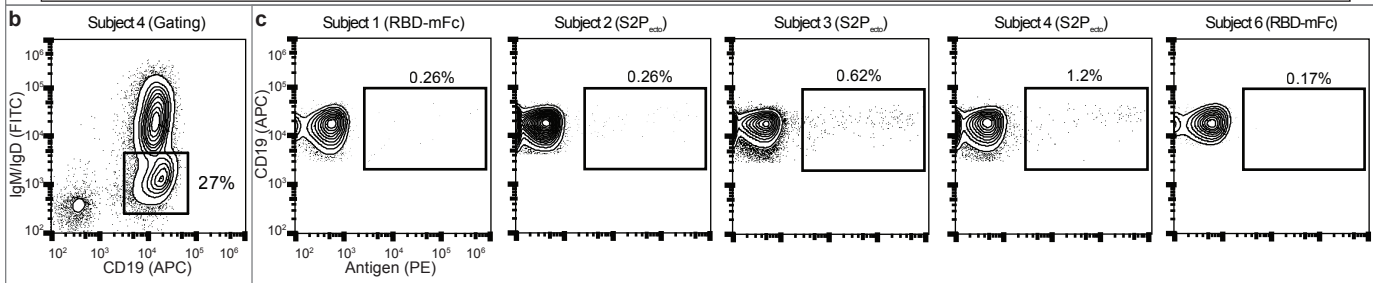
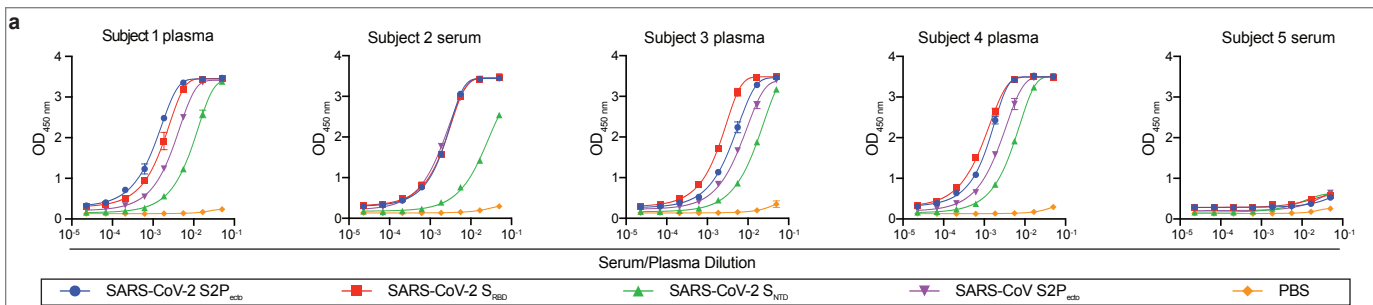
**310
reactive
mAbs**

Antigen reactivity

**76
reactive
mAbs**

Functional characterization





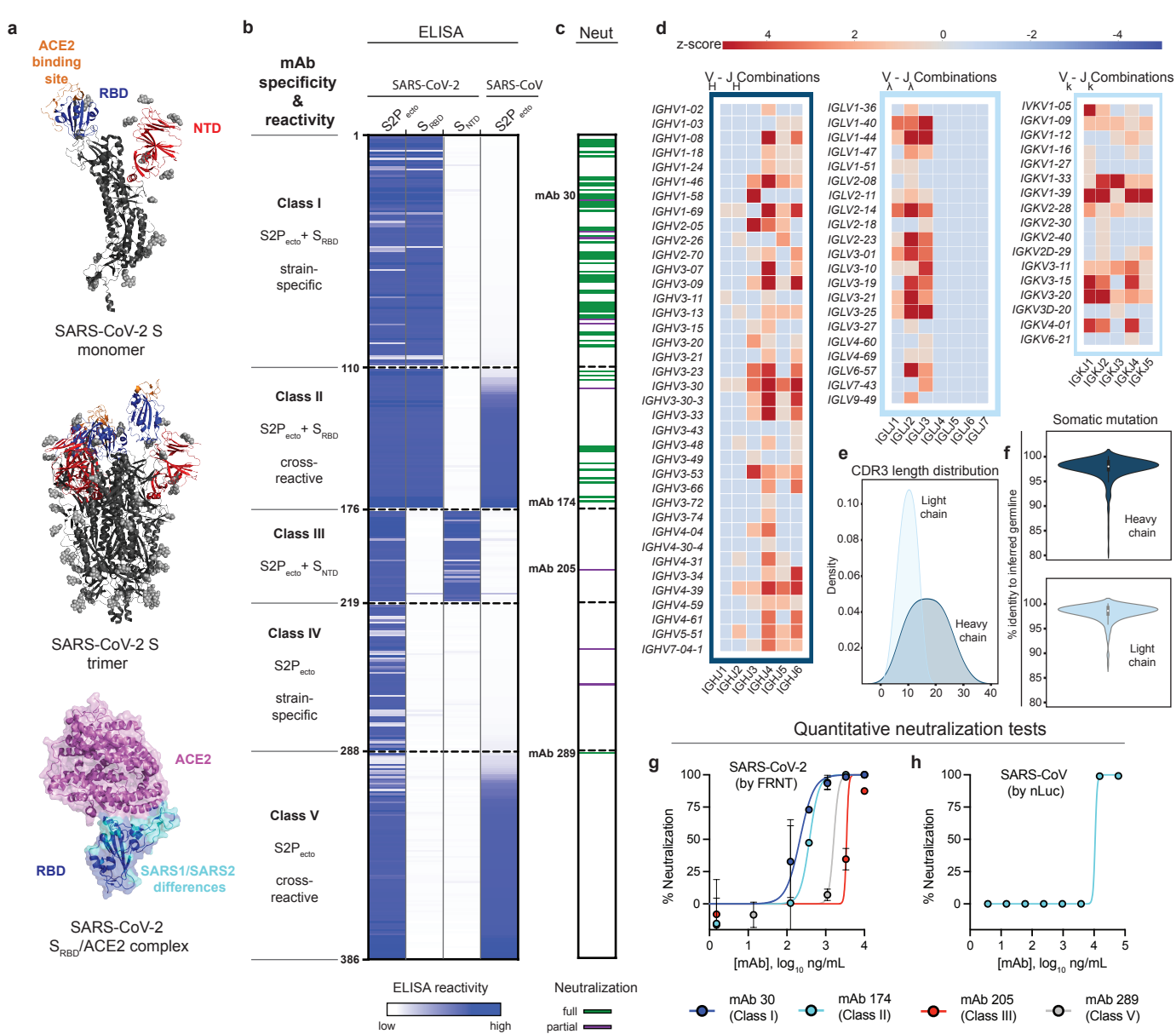
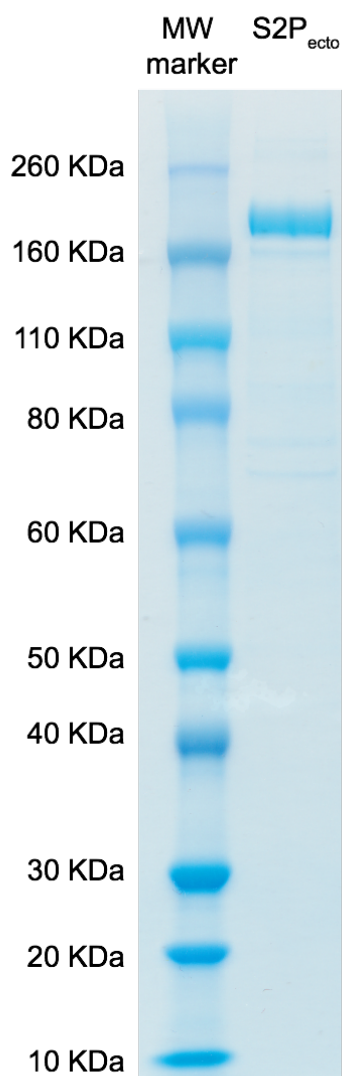
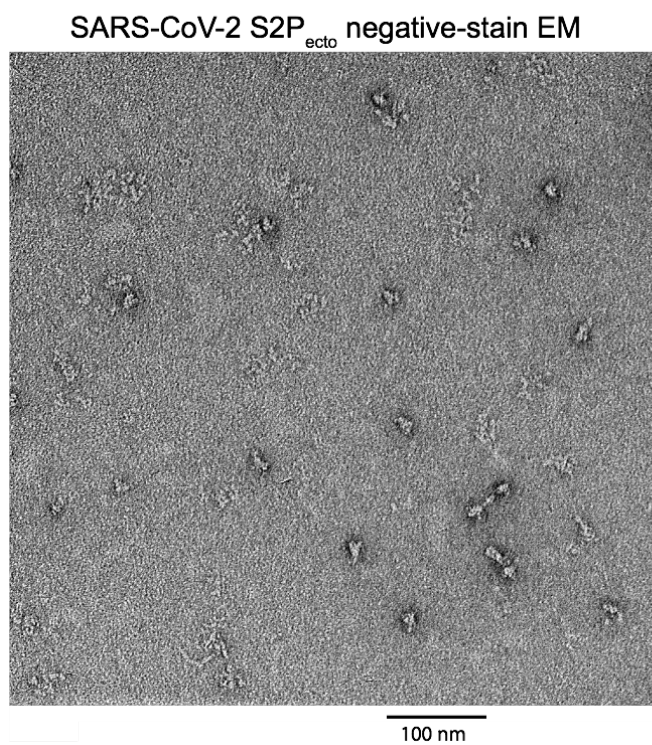


Figure S1

a



b



c

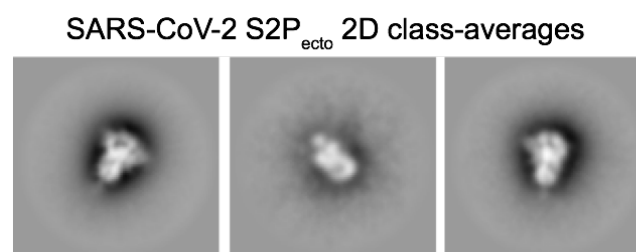


Figure S2

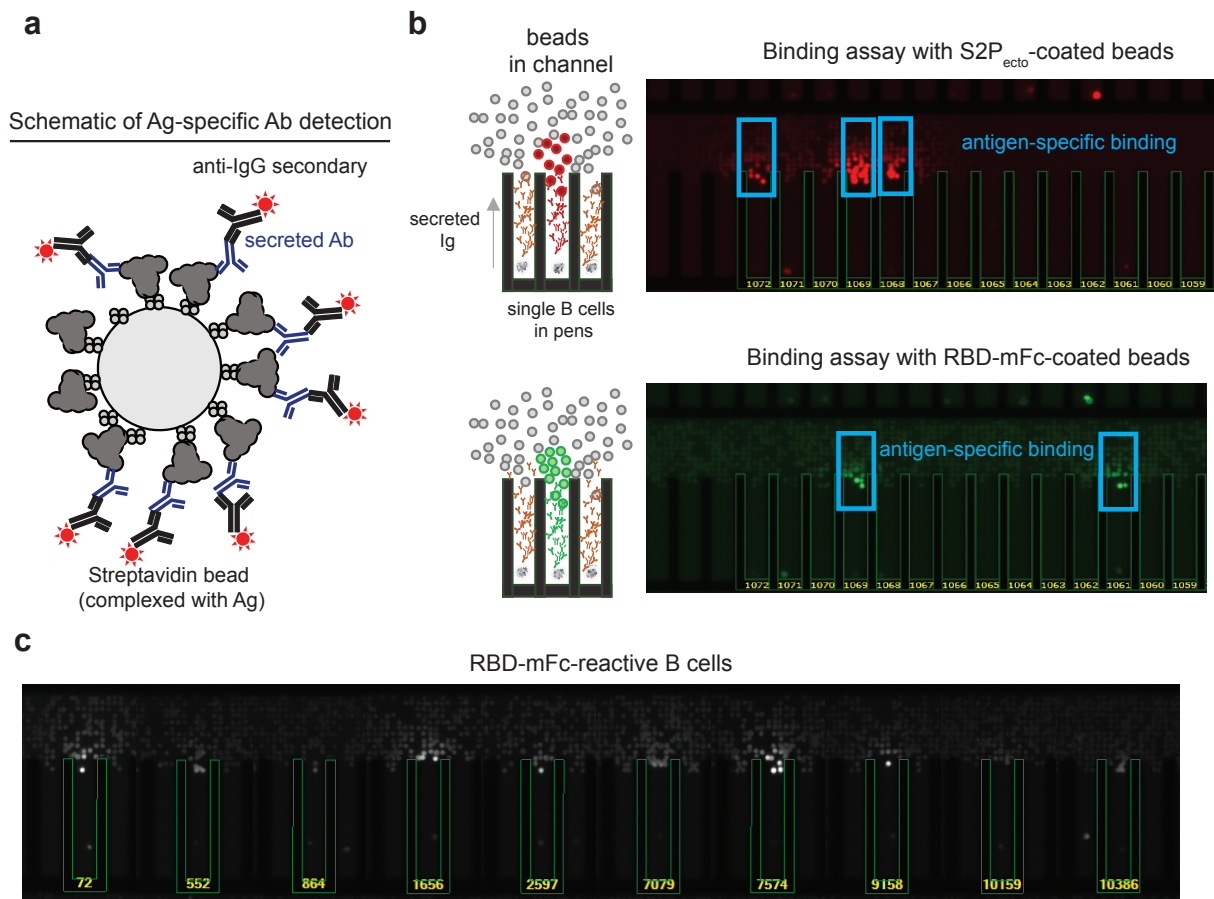
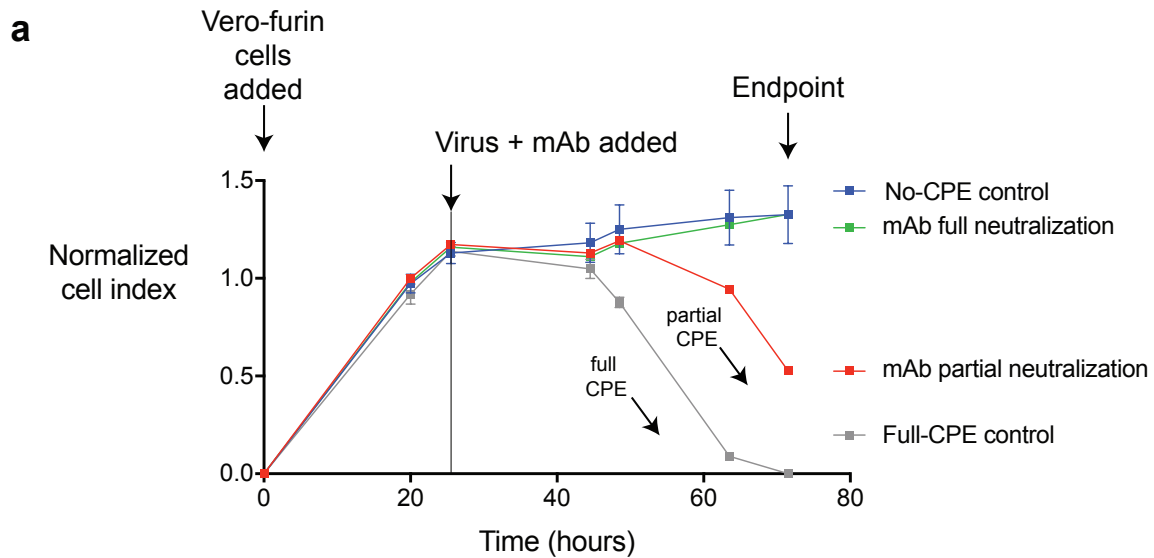
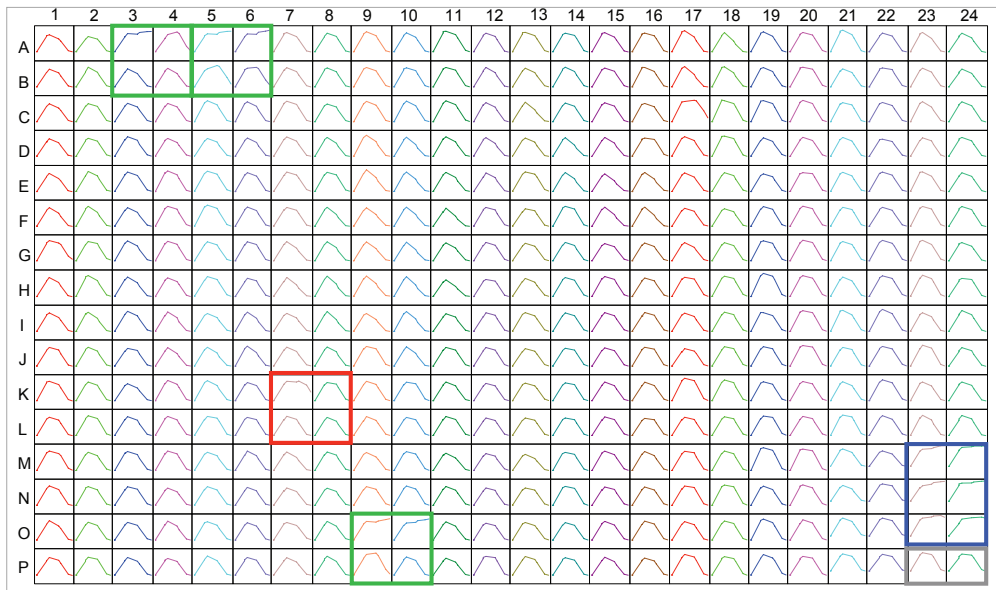


Figure S3



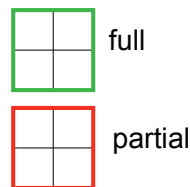
b Sensogram for cell impedance measurements over time, in 384-well plate assay



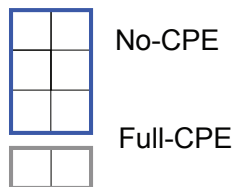
MAb
fold-dilution
schema

20	100
500	2,500

MAb neutralizing activity



Control wells



Supplemental Tables

Table S1. Human subjects studied in this paper						
Subject type	Subject	Age (years)	Sex	City where infected	Date of symptom onset	Date of blood sample collection (days after symptom onset)
COVID-19	1	35	M	Wuhan	Jan. 15, 2020	February 19, 2020 (35 days)
	2	52	F	Beijing	Feb. 1, 2020	March 8, 2020 (36 days)
	3	56	M	Wuhan	Jan. 20, 2020	March 10, 2020 (50 days)
	4	56	F	Wuhan	Jan. 20, 2020	March 10, 2020 (50 days)
Healthy donors	5	58	M	na	na	March 12, 2020 (na)
	6	Unknown	Unknown	na	na	Unknown, commercially sourced healthy donor sample

na, indicates not applicable

Table S2. Workflows used to isolate SARS-CoV-2 specific human mAbs from single B cells

Single B cell technique (number of Ag-reactive mAbs recovered)	Ag used for cell sorting	Feeder layer stimulation	Functional screen on instrument	Sequencing technique (cDNA used)	Expression construct
Beacon (n = 76)	S2P _{ecto +/-} S _{RBD}	+	S2P _{ecto} binding	PacBio SMRT (PCR amplicon)	Directly cloned cDNA in pMCis_G1 vector
			RBD-mFc binding		
			RBD-mFc binding + ACE2 blocking		
Chromium (n = 310)	S2P _{ecto}	+	na	Illumina Novaseq (Chromium libraries)	Synthesized cDNA in pTwist-mCis_G1 vector
		-			
	S _{RBD}	+			
		-			

Table S3. Summary of electron microscopy data collection and statistics SARS-CoV-2 S2P_{ecto} protein		
Microscope setting	Microscope	TF-20
	Voltage (kV)	200
	Detector	US-4000 CCD
	Magnification	50,000×
	Pixel size	2.18
	Exposure (e ⁻ /Å ²)	25
	Defocus range (μm)	1.5 to 1.8
Data	Micrographs, #	122
	Particles, #	3,836
	Particles, # after 2D	2,718
	Final particles, #	2,188
	Symmetry	C1
Model docking		PDB: 6VXX
	CoV-2 S CC	0.895

1 **Online Methods**

2

3 **Research subjects.** We studied four subjects in North America with recent laboratory-

4 confirmed symptomatic SARS-CoV-2 infection that were acquired in China (**Table S1**). The

5 studies were approved by the Institutional Review Board of Vanderbilt University Medical

6 Center, and subsite studies were approved by the Institutional Review Board of the

7 University of Washington or the Research Ethics Board of the University of Toronto. Samples

8 were obtained after written informed consent. Subject 1 (35-year-old male) was the earliest

9 reported case of SARS-CoV-2 infection in the U.S. who presented with disease in Seattle, WA

10 on January 19, 2020¹, a blood sample was obtained for study on February 19, 2020. Subject 2

11 (52-year-old female) was infected following close exposure in Beijing, China to an infected

12 person from Wuhan, China during the period between January 23 to January 29, 2020. She

13 presented with mild respiratory disease symptoms from February 1 to 4, 2020 that occurred

14 after travel to Madison, Wisconsin, USA. She obtained a diagnosis of infection by testing at

15 the U.S. Centers for Disease Control on February 5, 2020. Blood samples were obtained for

16 study on March 7 and March 8, 2020. Subject 3 (a 56-year-old male) and subject 4 (a 56-year-

17 old female) are a married couple and residents of Wuhan, China who traveled to Toronto,

18 Canada on January 22, 2020. Subject 3 first developed a cough without fever on January 20,

19 2020 in the city of Wuhan, where he had a normal chest x-ray on that day. He flew to Canada

20 with persisting cough and arrived in Canada January 22, 2020 where he became febrile. He

21 presented to a hospital in Toronto, January 23, 2020 complaining of fever, cough and

22 shortness of breath; a nasopharyngeal swab was positive by PCR testing for SARS-CoV-2. His

23 chest x-ray at that time was abnormal, and he was admitted for non-ICU inpatient care. He

24 improved gradually with supportive care, was discharged January 30, 2020 and rapidly

25 became asymptomatic except for a residual dry cough that persisted for a month. He had a

26 negative nasopharyngeal swab PCR test on February 19, 2020. Subject 4 is the wife of subject 3
27 who traveled with her husband from Wuhan. She was never symptomatic with respiratory
28 symptoms or fever but was tested because of her exposure. Her nasopharyngeal swab was
29 positive for SARS-CoV-2 by PCR, on January 24, 2020; repeat testing in followup on February
30 21, 2020 was negative. PBMCs were obtained by leukopheresis from subjects 3 and 4 on
31 March 10, 2020, which was 50 days since the symptom onset of subject 3. Samples were
32 transferred to Vanderbilt University Medical Center in Nashville, TN, USA on March 14,
33 2020.

34
35 **Cell culture.** Vero E6 (CRL-1586, American Type Culture Collection (American Type
36 Culture Collection, ATCC), Vero CCL81 (ATCC), HEK293 (ATCC), and HEK293T
37 (ATCC) were maintained at 37°C in 5% CO₂ in Dulbecco's minimal essential medium
38 (DMEM) containing 10% (vol/vol) heat-inactivated fetal bovine serum (FBS), 10 mM
39 HEPES pH 7.3, 1 mM sodium pyruvate, 1× non-essential amino acids, and 100 U/mL of
40 penicillin–streptomycin. Vero-furin cells were obtained from T. Pierson (NIH) and have
41 been described previously². Expi293F cells (ThermoFisher Scientific, A1452) were
42 maintained at 37°C in 8% CO₂ in Expi293F Expression Medium (ThermoFisher
43 Scientific, A1435102). ExpiCHO cells (ThermoFisher Scientific, A29127) were
44 maintained at 37°C in 8% CO₂ in ExpiCHO Expression Medium (ThermoFisher
45 Scientific, A2910002). Mycoplasma testing of Expi293F and ExpiCHO cultures was
46 performed on a monthly basis using a PCR-based mycoplasma detection kit (ATCC, 30-
47 1012K).

48
49 **Viruses.** SARS-CoV-2 strain 2019 n-CoV/USA_WA1/2020 was obtained from the Centers for
50 Disease Control and Prevention (a gift from Natalie Thornburg). Virus was passaged in Vero

51 CCL81 cells and titrated by plaque assay on Vero E6 cells. All work with infectious SARS-
52 CoV-2 was approved by the Washington University School of Medicine or UNC-Chapel Hill
53 Institutional Biosafety Committees and conducted in approved BSL3 facilities using
54 appropriate powered air purifying respirators and personal protective equipment.

55
56 **Recombinant antigens and proteins.** A gene encoding the ectodomain of a prefusion
57 conformation-stabilized SARS-CoV-2 spike ($S2P_{\text{ecto}}$) protein was synthesized and cloned into a
58 DNA plasmid expression vector for mammalian cells. A similarly designed S protein antigen
59 with two prolines and removal of the furin cleavage site for stabilization of the prefusion form
60 of S was reported previously³. Briefly, this gene includes the ectodomain of SARS-CoV-2 (to
61 residue 1,208), a T4 fibritin trimerization domain, an AviTag site-specific biotinylation
62 sequence, and a C-terminal 8x-His tag. To stabilize the construct in the prefusion
63 conformation, we included substitutions K968P and V969P and mutated the furin cleavage
64 site at residues 682-685 from RRAR to ASVG. This recombinant spike 2P-stabilized protein
65 (designated here as $S2P_{\text{ecto}}$) was isolated by metal affinity chromatography on HisTrap Excel
66 columns (GE Healthcare), and protein preparations were purified further by size-exclusion
67 chromatography on a Superose 6 Increase 10/300 column (GE Healthcare). The presence of
68 trimeric, prefusion conformation S protein was verified by negative-stain electron microscopy
69 (**Figure S1**). To express the S_{RBD} subdomain of SARS-CoV-2 S protein, residues 319-541 were
70 cloned into a mammalian expression vector downstream of an IL-2 signal peptide and
71 upstream of a thrombin cleavage site, an AviTag, and a 6x-His tag. RBD protein fused to
72 mouse IgG1 Fc domain (designated RBD-mFc), was purchased from Sino Biological (40592-
73 V05H). For B cell labeling and sorting, RBD-mFc and $S2P_{\text{ecto}}$ proteins were biotinylated using
74 the EZ-Link™ Sulfo-NHS-LC-Biotinylation Kit and vendor's protocol (ThermoFisher
75 Scientific, 21435).

76

77 **Electron microscopy (EM) stain grid preparation and imaging of SARS-CoV-2 S2P_{ecto}**
78 **protein.** For screening and imaging of negatively-stained (NS) SARS-CoV-2 S2P_{ecto}
79 protein, approximately 3 μ L of the sample at concentrations of about 10 to 15 μ g/mL
80 was applied to a glow discharged grid with continuous carbon film on 400 square mesh
81 copper EM grids (Electron Microscopy Sciences, Hatfield, PA). The grids were stained
82 with 0.75% uranyl formate (UF)⁴. Images were recorded on a Gatan US4000 4k \times 4k
83 CCD camera using an FEI TF20 (TFS) transmission electron microscope operated at 200
84 keV and control with SerialEM⁵. All images were taken at 50,000 \times magnification with a
85 pixel size of 2.18 \AA /pix in low-dose mode at a defocus of 1.5 to 1.8 μ m. Total dose for
86 the micrographs was $\sim 25 \text{ e}^- / \text{\AA}^2$. Image processing was performed using the
87 cryoSPARC software package⁶. Images were imported, and particles were CTF
88 estimated. The images then were denoised and picked with Topaz⁷. The particles were
89 extracted with a box size of 256 pixels and binned to 128 pixels. 2D class averages were
90 performed and good classes selected for *ab-initio* model and refinement without
91 symmetry (see also **Table S3** for details). For EM model docking of SARS-CoV-2 S2P_{ecto}
92 protein, the closed model (PDB: 6VXX) was used in Chimera⁸ for docking to the EM
93 map (see also **Table S3** for details).

94

95 **Human subject selection and target-specific memory B cells isolation.** B cell responses to
96 SARS-CoV-2 in PBMCs from a cohort of four subjects with documented previous infection
97 with the virus were analyzed for antigen specificity, and PBMCs were used for SARS-CoV-2-
98 specific B cell enrichment. The frequency of SARS-CoV-2 S protein-specific B cells was
99 identified by antigen-specific staining with either biotinylated S2P_{ecto} or RBD-mFc protein.

100 Briefly, B cells were purified magnetically (STEMCELL Technologies) and stained with anti-
101 CD19-APC (clone HIB19, 982406), -IgD-FITC (clone LA6-2, 348206), and -IgM-FITC (clone
102 MNM-88, 314506) phenotyping antibodies (BioLegend) and biotinylated antigen. A 4',6-
103 diamidino-2-phenylindole (DAPI) stain was used as a viability dye to discriminate dead cells.
104 Antigen-labeled class-switched memory B cell-antigen complexes (CD19⁺IgM⁺IgD⁺Ag⁺DAPI⁺)
105 were detected with a R-phycoerythrin (PE)-labeled streptavidin conjugate (ThermoFisher
106 Scientific, S866). After identification of the two subjects with the highest B cell response
107 against SARS-CoV-2 (subjects 3 and 4), target-specific memory B cells were isolated by flow
108 cytometric sorting using an SH800 cell sorter (Sony) from pooled PBMCs of these two
109 subjects, after labeling of B cells with either biotinylated S2P_{ecto} or RBD-mFc proteins.

110
111 Overall, from $> 4 \times 10^8$ PBMCs, 2,126 RBD-mFc-reactive and 5,544 S2P_{ecto} protein-reactive B
112 cells were sorted and subjected to further analysis. Several methods were implemented for the
113 preparation of sorted B cells for sequencing. Approximately 4,500 sorted cells were subjected
114 to direct sequencing immediately after flow cytometric sorting. The remaining cells were
115 expanded in culture for eight days in the presence of irradiated 3T3 feeder cells that were
116 engineered to express human CD40L, IL-21, and BAFF, as described previously⁹. The
117 expanded lymphoblastoid cell lines (LCLs) secreted high levels of S protein-specific
118 antibodies, as confirmed by ELISA to detect antigen-specific human antibodies in culture
119 supernatants. Approximately 40,000 expanded LCLs were sequenced using the Chromium
120 sequencing method (10x Genomics).

121
122 **Microfluidic device selection of single antigen-specific B cells.** Activated memory B
123 cells were screened using Berkeley Lights' Beacon[®]™ optofluidic system. Purified B cell
124 samples were imported automatically onto OptoSelect™ 11k chips in a novel

125 plasmablast survival medium that promotes antibody secretion and preserves cell
126 viability¹⁰. Single-cell penning was then performed using OEP™ technology in which
127 light is used to transfer B cells into individual nanoliter-volume chambers
128 (NanoPens™). Using this light-based manipulation, thousands of LCLs were
129 transferred into pens across multiple chips in each workflow. We performed an on-chip,
130 fluorescence-based assay to identify antibodies that bound SARS-CoV-2 S2P_{ecto} or RBD-
131 mFc protein. We prepared 6- to 8-micron and 10- to 14-micron RBD-mFc-conjugated
132 beads by coupling biotinylated RBD-mFc protein to streptavidin-coated polystyrene
133 particles (Spherotech Inc.). We prepared 6- to 8-micron S2P_{ecto} protein-conjugated beads
134 by coupling full-length S2P_{ecto} protein to streptavidin-coated polystyrene particles.
135 Assays consisted of mixing beads conjugated with the RBD-mFc or S2P_{ecto} proteins with
136 fluorescently-labeled anti-human secondary antibodies (AF568, Thermo Fisher
137 Scientific) and importing this assay mixture into OptoSelect 11k chips. Antigen-specific
138 antibodies bound the antigen-conjugated beads, which then sequestered the fluorescent
139 secondary antibody. Cells secreting antigen-specific antibodies were identified by
140 locating the NanoPens immediately adjacent to the fluorescent beads. Antigen-specific
141 cells of interest were exported from specific NanoPen chambers to individual wells of
142 96-well RT-PCR plates containing lysis buffer.

143
144 **Sequencing and cloning of single antigen-specific B cells.** After export from the Beacon,
145 antibody heavy and light chain sequences for B cells secreting antibodies with RBD-mFc- or
146 S2P_{ecto}-binding antibodies were amplified and recovered using components of the
147 Opto™ Plasma B Discovery cDNA Synthesis Kit (Berkeley Lights). Antibody heavy and light
148 chain sequences were amplified through a 5'RACE approach using the kit's included "BCR
149 Primer 2" forward primer and isotype-specific reverse primers. The 5'-RACE amplified cDNA

150 was sequenced using the Pacific Biosciences Sequel platform using the SMRTbell Barcoded
151 Adapt Complete Prep-96 kit (Pacific Biosciences) and a 6-hour movie time. In a redundant
152 sequencing approach, heavy and light chain sequences were amplified using a cocktail of
153 custom V and J gene-specific primers (similar to previously described human Ig gene-specific
154 primers¹¹) from the original 5'-RACE-amplified cDNA while the products of the gene-specific
155 amplification were sent for Sanger sequencing (GENEWIZ). The sequences generated by these
156 two approaches were analyzed using our Python-based antibody variable gene analysis tool
157 (PyIR; <https://github.com/crowelab/PyIR>)¹² to identify which V and J genes most closely
158 matched the nucleotide sequence. Heavy and light chain sequences were then amplified from
159 the original cDNA using cherry-picked V and J gene-specific primers most closely
160 corresponding to the V and J gene calls made by PyIR. These primers include adapter
161 sequences which allow Gibson-based cloning into a monocistronic IgG1 expression vector
162 (pMCis_G1). Similar to a vector described below, this vector contains an enhanced 2A
163 sequence and GSG linker that allows simultaneous expression of mAb heavy and light chain
164 genes from a single construct upon transfection¹³. The pMCis_G1 vector was digested using
165 the New England BioLabs restriction enzyme FspI, and the amplified paired heavy and light
166 chain sequences were cloned through Gibson assembly using NEBuilder HiFi DNA Assembly
167 Master Mix. After recovered sequences were cloned into pMCis_G1 expression constructs,
168 recombinant antibodies were expressed in Chinese hamster ovary (CHO) cells and purified
169 by affinity chromatography as detailed below. Antigen-binding activity was confirmed using
170 plate-based ELISA.

171
172 **Generation of single-cell antibody variable genes profiling libraries.** As an alternative
173 approach, we also used a second major approach for isolation of SARS-CoV-2-reactive
174 antibodies. In some experiments, the Chromium Single Cell V(D)J workflow with B-cell only

175 enrichment option was used for generating linked heavy-chain and light-chain antibody
176 profiling libraries. Approximately 2,866 directly sorted S2P_{ecto} or 1,626 RBD-mFc protein-
177 specific B cells were split evenly into two replicates each and separately added to 50 µL of RT
178 Reagent Mix, 5.9 µL of Poly-dt RT Primer, 2.4 µL of Additive A and 10 µL of RT Enzyme Mix
179 B to complete the Reaction Mix as per the vendor's protocol, which then was loaded directly
180 onto a Chromium chip (10x Genomics). Similarly, for the remaining sorted cells that were
181 expanded in bulk, approximately 40,000 cells from two separate sorting approaches were split
182 evenly across four reactions and processed separately as described above before loading onto
183 a Chromium chip. The libraries were prepared following the User Guide for Chromium
184 Single Cell V(D)J Reagents kits (CG000086_REV C).

185
186 **Next generation DNA sequence analysis of antibody variable genes.** Chromium Single Cell
187 V(D)J B-Cell enriched libraries were quantified, normalized and sequenced according to the
188 User Guide for Chromium Single Cell V(D)J Reagents kits (CG000086_REV C). The two
189 enriched libraries from direct flow cytometric cell sorting were sequenced on a NovaSeq
190 sequencer (Illumina) with a NovaSeq 6000 S1 Reagent Kit (300 cycles) (Illumina). The four
191 enriched libraries from bulk expansion were sequenced on a NovaSeq sequencer with a
192 NovaSeq 6000 S4 Reagent Kit (300 cycles (Illumina). All enriched V(D)J libraries were targeted
193 for sequencing depth of at least 5,000 raw read pairs per cell. Following sequencing, all
194 samples were demultiplexed and processed through the 10x Genomics Cell Ranger software
195 (version 2.1.1) as below.

196
197 **Bioinformatics analysis of single-cell sequencing data.** The down-selection to identify lead
198 candidates for expression was carried out in two phases. In the first phase, all paired antibody
199 heavy and light chain variable gene cDNA nucleotide sequences obtained that contained a

200 single heavy and light chain sequence were processed using PyIR. We considered heavy and
201 light chain encoding gene pairs productive and retained them for additional downstream
202 processing if they met the following criteria: 1) did not contain a stop codon, 2) encoded an
203 intact CDR3 and 3) contained an in-frame junctional region. The second phase of processing
204 eliminated redundant sequences (those with identical amino acid sequences). Any antibody
205 variant that was designated as an IgM isotype (based on the sequence and assignment using
206 the 10x Genomics Cell Ranger V(D)J software [version 2.1.1]) was removed from
207 consideration (while IgG and IgA isotype antibodies were retained). The identities of
208 antibody variable gene segments, CDRs, and mutations from inferred germline gene
209 segments were determined by using PyIR.

210
211 **Antibody gene synthesis.** Sequences of selected mAbs were synthesized using a rapid high-
212 throughput cDNA synthesis platform (Twist Bioscience) and subsequently cloned into an
213 IgG1 monocistronic expression vector (designated as pTwist-mCis_G1) for mammalian cell
214 culture mAb secretion. This vector contains an enhanced 2A sequence and GSG linker that
215 allows simultaneous expression of mAb heavy and light chain genes from a single construct
216 upon transfection¹³.

217
218 **MAb production and purification.** For high-throughput production of recombinant mAbs,
219 we adopted approaches designated as “micro-scale” or “midi-scale”. For “micro-scale”
220 mAbs expression, we performed micro-scale transfection (~1 mL per antibody) of CHO cell
221 cultures using the Gibco™ ExpiCHO™ Expression System and a protocol for deep 96-well
222 blocks (ThermoFisher Scientific) as detailed in accompanying manuscript¹⁴. Briefly,
223 synthesized antibody-encoding lyophilized DNA was reconstituted in OptiPro serum-free
224 medium (OptiPro SFM) and used for transfection of ExpiCHO cell cultures into 96-deep-

225 well blocks. For high-throughput micro-scale mAbs purification, clarified culture
226 supernatants were incubated with MabSelect SuRe resin (Cytiva, formerly GE Healthcare
227 Life Sciences), washed with PBS, eluted, buffer-exchanged into PBS using Zeba™ Spin
228 Desalting Plates (Thermo Fisher Scientific) and stored at 4°C until use. For “midi-scale”
229 mAbs expression, we performed transfection (~15 mL per antibody) of CHO cell cultures
230 using the Gibco™ ExpiCHO™ Expression System and protocol for 50 mL mini bioreactor
231 tubes (Corning) as described by the vendor. For high-throughput midi-scale mAb
232 purification, culture supernatants were purified using HiTrap MabSelect SuRe (Cytiva,
233 formerly GE Healthcare Life Sciences) on a 24-column parallel protein chromatography
234 system (Protein BioSolutions). Purified mAbs were buffer-exchanged into PBS,
235 concentrated using Amicon® Ultra-4 50KDa Centrifugal Filter Units (Millipore Sigma) and
236 stored at 4°C until use.

237
238 **ELISA binding screening assays.** Wells of 96-well microtiter plates were coated with
239 purified recombinant SARS-CoV-2 S protein, SARS-CoV-2 S_{RBD} protein, SARS-CoV-2 S_{NTD}
240 (kindly provided by Nicole Kallewaard-Lelay, Astra Zeneca) or SARS-CoV S protein
241 (kindly provided by Sandhya Bangaru and Andrew Ward, The Scripps Research Institute)
242 at 4°C overnight. Plates were blocked with 2% non-fat dry milk and 2% normal goat serum
243 in DPBS containing 0.05% Tween-20 (DPBS-T) for 1 hr. For mAb screening assays, CHO cell
244 culture supernatants or purified mAbs were diluted 1:20 in blocking buffer, added to the
245 wells, and incubated for 1 hr at ambient temperature. The bound antibodies were detected
246 using goat anti-human IgG conjugated with HRP (horseradish peroxidase) (Southern
247 Biotech) and TMB (3,3',5,5'-tetramethylbenzidine) substrate (Thermo Fisher Scientific).
248 Color development was monitored, 1N hydrochloric acid was added to stop the reaction,

249 and the absorbance was measured at 450 nm using a spectrophotometer (Biotek). For dose-
250 response assays, serial dilutions of purified mAbs were applied to the wells in triplicate,
251 and mAb binding was detected as detailed above. Half-maximal effective concentration
252 (EC_{50}) values for binding were determined using Prism v8.0 software (GraphPad) after log
253 transformation of mAb concentration using sigmoidal dose-response nonlinear regression
254 analysis.

255
256 **Real-time cell analysis assay (RTCA).** To screen for neutralizing activity in the panel of
257 recombinantly expressed mAbs, we used a high-throughput and quantitative real-time cell
258 analysis (RTCA) assay and xCelligence RTCA HT Analyzer (ACEA Biosciences Inc.) that
259 assesses kinetic changes in cell physiology, including virus-induced cytopathic effect
260 (CPE). Twenty (20) μ L of cell culture medium (DMEM supplemented with 2% FBS) was
261 added to each well of a 96-well E-plate using a ViaFlo384 liquid handler (Integra
262 Biosciences) to obtain background reading. Six thousand (6,000) Vero-furin cells in 20 μ L of
263 cell culture medium were seeded per each well, and the plate was placed on the analyzer.
264 Sensograms were visualized using RTCA HT software version 1.0.1 (ACEA Biosciences
265 Inc). For a screening neutralization assay, equal amounts of virus were mixed with micro-
266 scale purified Abs in a total volume of 40 μ L using DMEM supplemented with 2% FBS as a
267 diluent and incubated for 1 hr at 37°C in 5% CO₂. At ~17-20 hrs after seeding the cells, the
268 virus-mAb mixtures were added to the cells in 384-well E-plates. Wells containing virus
269 only (in the absence of mAb) and wells containing only Vero cells in medium were
270 included as controls. Plates were measured every 8-12 hours for 48 to 72 hrs to assess virus
271 neutralization. Micro-scale antibodies were assessed in four 5-fold dilutions (starting from
272 a 1:20 sample dilution), and their concentrations were not normalized. In some experiments

273 mAbs were tested in triplicate using a single (1:20) dilution. Neutralization was calculated
274 as the percent of maximal cell index in control wells without virus minus cell index in
275 control (virus-only) wells that exhibited maximal CPE at 40 to 48 hrs after applying virus-
276 antibody mixture to the cells. A mAb was classified as fully neutralizing if it completely
277 inhibited SARS-CoV-2-induced CPE at the highest tested concentration, while a mAb was
278 classified as partially neutralizing if it delayed but did not fully prevent CPE at the highest
279 tested concentration. Representative sensograms for fully neutralizing and partially
280 neutralizing mAbs are shown in Figure S3. For mAb potency ranking experiments,
281 individual mAbs identified as fully neutralizing from the screening study were assessed by
282 FRNT.

283

284 **Sequence analysis of antigen-reactive mAb sequences.** Sequences of the 386 mAbs
285 isolated by different approaches were combined and run through PyIR to identify the V
286 genes, J genes, CDR3 lengths, and percent identity to germline, and sequence within the
287 FR1-FR4 region for both heavy and light chains. Sequences were then deduplicated on
288 the nucleotide sequences identified in the FR1-FR4 region. Among the 386 mAbs, there
289 were 324 unique nucleotide sequences that were analyzed for V/D/J gene usage, CDR3
290 length, and somatic mutation. First, the number of sequences with corresponding V and
291 J genes were counted. The V/J frequency counts were then transformed into a z-score
292 by first subtracting away the average frequency then normalizing by the standard
293 deviation of each subject. The z-score was then plotted as a heatmap using python
294 seaborn library. The amino acid length of each CDR3 was counted. The distribution of
295 CDR3 amino acid lengths were then plotted as histograms and fitted using kernel
296 density estimation for the curves using python seaborn library. The number of
297 mutations from each inferred germ-line sequence starting from FR-1 to FR4 was

298 counted up for each chain. This number was then transformed into a percentage value.
299 These values are then plotted as a categorical distribution plot as a violin plot using the
300 python seaborn.catplot library.

301

302 **Focus reduction neutralization test (FRNT).** Serial dilutions of mAbs were incubated
303 with 10^2 FFU of SARS-CoV-2 for 1 hr at 37°C. The mAb–virus complexes were added to
304 Vero E6 cell monolayers in 96-well plates for 1 hr at 37°C. Subsequently, cells were
305 overlaid with 1% (w/v) methylcellulose in Minimum Essential Medium (MEM)
306 supplemented to contain 2% heat-inactivated FBS. Plates were fixed 30 hrs later by
307 removing overlays and fixed with 4% PFA in PBS for 20 min at room temperature. The
308 plates were incubated sequentially with 1 $\mu\text{g}/\text{mL}$ of rCR3022 anti-S antibody¹⁵ and
309 horseradish-peroxidase (HRP)-conjugated goat anti-human IgG in PBS supplemented
310 with 0.1% (w/v) saponin (Sigma) and 0.1% bovine serum albumin (BSA). SARS-CoV-2-
311 infected cell foci were visualized using TrueBlue peroxidase substrate (KPL) and
312 quantitated on an ImmunoSpot 5.0.37 Macro Analyzer (Cellular Technologies).

313

314 **SARS-CoV neutralization assays using SARS-CoV luciferase reporter virus.** Full-
315 length viruses expressing luciferase were designed and recovered via reverse genetics
316 and described previously.^{16,17} Viruses were titered in Vero E6 USAMRID cell culture
317 monolayers to obtain a relative light units (RLU) signal of at least 20X the cell-only
318 control background. Vero E6 USAMRID cells were plated at 20,000 cells per well the
319 day prior in clear-bottom black-walled 96-well plates (Corning #3904). Neutralizing
320 antibodies were diluted serially 4-fold up to eight dilution times. SARS-Urbani
321 NanoLuc virus was mixed with serially diluted antibodies. Antibody-virus complexes
322 were incubated at 37°C in 5% CO₂ for 1 hr. Following incubation, growth medium was

323 removed and virus-antibody dilution complexes were added to the cells in duplicate.
324 Virus-only and cell-only controls were included in each neutralization assay plate.
325 Following infection, plates were incubated at 37°C in 5% CO₂ for 48 hours. After the 48-
326 hour incubation, cells were lysed and luciferase activity was measured using the Nano-
327 Glo Luciferase Assay System (Promega), according to the manufacturer's specifications.
328

329 **High-throughput mAb quantification.** High-throughput quantification of micro-scale
330 produced mAbs was performed from CHO culture supernatants or micro-scale purified
331 mAbs in a 96-well plate format using the Cy-Clone Plus Kit and an iQue Plus Screener flow
332 cytometer (IntelliCyt Corp), according to the vendor's protocol. Purified mAbs were assessed
333 at a single dilution (1:10 final, using 2 µL of purified mAb per reaction), and a control human
334 IgG solution with known concentration was used to generate a calibration curve. Data were
335 analyzed using ForeCyt software version 6.2 (IntelliCyt Corp).

336
337 **Quantification and statistical analysis.** The descriptive statistics mean ± SEM or mean ±
338 SD were determined for continuous variables as noted. Technical and biological replicates
339 are described in the figure legends. Statistical analyses were performed using Prism v8.0
340 (GraphPad).

341
342

343 **References for Online Methods**

344

345 1. Holshue, M.L., *et al.* First case of 2019 novel coronavirus in the United States. *N*
346 *Engl J Med* **382**, 929-936 (2020).

347

348 2. Mukherjee, S., *et al.* Enhancing dengue virus maturation using a stable furin
349 over-expressing cell line. *Virology* **497**, 33-40 (2016).

350

351 3. Wrapp, D., *et al.* Cryo-EM structure of the 2019-nCoV spike in the prefusion
352 conformation. *Science* **367**, 1260-1263 (2020).

353

354 4. Ohi, M., Li, Y., Cheng, Y. & Walz, T. Negative staining and image classification -
355 Powerful tools in modern electron microscopy. *Biol Proced Online* **6**, 23-34 (2004).

356

357 5. Mastronarde, D.N. Automated electron microscope tomography using robust
358 prediction of specimen movements. *J Struct Biol* **152**, 36-51 (2005).

359

360 6. Punjani, A., Rubinstein, J.L., Fleet, D.J. & Brubaker, M.A. cryoSPARC: algorithms
361 for rapid unsupervised cryo-EM structure determination. *Nat Methods* **14**, 290-296
362 (2017).

363

364 7. Bepler, T., Noble, A. J., and Berger, B. Topaz-Denoise: general deep denoising
365 models for cryoEM. *bioRxiv*. (2019). DOI: 10.1101/838920

366

- 367 8. Pettersen, E.F., *et al.* UCSF Chimera--a visualization system for exploratory
368 research and analysis. *J Comput Chem* **25**, 1605-1612 (2004).
369
- 370 9. Gilchuk, P., *et al.* Analysis of a therapeutic antibody cocktail reveals determinants
371 for cooperative and broad ebolavirus neutralization. *Immunity* **52**, 388-403 e312
372 (2020).
373
- 374 10. Nguyen, D.C., *et al.* Factors of the bone marrow microniche that support human
375 plasma cell survival and immunoglobulin secretion. *Nat Commun* **9**, 3698 (2018).
376
- 377 11. Guthmiller, J.J., Dugan, H.L., Neu, K.E., Lan, L.Y. & Wilson, P.C. An efficient
378 method to generate monoclonal antibodies from human B cells. *Methods Mol Biol*
379 **1904**, 109-145 (2019).
380
- 381 12. Soto C, F.J., Willis JR, Day SB, Sinkovits RS, Jones T, Schmitz S, Meiler J,
382 Branchizio A, Crowe JE Jr. . PyIR: A scalable wrapper for processing billions of
383 immunoglobulin and T cell receptor sequences using IgBLAST. (2020). *Submitted*.
384
- 385 13. Chng, J., *et al.* Cleavage efficient 2A peptides for high level monoclonal antibody
386 expression in CHO cells. *MAbs* **7**, 403-412 (2015).
387
- 388 14. Gilchuk P, B.R., Erasmus JH, Durnel LA, Nargi R, Soto C, Abbink P, Suscovich
389 TJ, Tan Q, Khandhar A, Archer J, Bryan A, Davidson E, Doranz BJ, Fouch ME,
390 Jones T, Larson E, Ertel S, Granger B, Fuerte-Stone J, Roy V, Broge T, Linnekin
391 TC, Linde CH, Gorman MJ, Nkolola J, Galit Alter G, Steven G Reed SG, Daniel H

- 392 Barouch DH, Michael S Diamond MS, Crowe JE Jr, Neal Hoeven N, Thackray L,
393 Carnahan R. Integrated technology platform for accelerated discovery of
394 antiviral antibody therapeutics. *Nature Medicine* (2020). *Submitted*.
395
- 396 15. Yuan, M., *et al.* A highly conserved cryptic epitope in the receptor binding
397 domains of SARS-CoV-2 and SARS-CoV. *Science* **368**, 630-633 (2020).
398
- 399 16. Scobey, T., *et al.* Reverse genetics with a full-length infectious cDNA of the
400 Middle East respiratory syndrome coronavirus. *Proc Natl Acad Sci U S A* **110**,
401 16157-16162 (2013).
402
- 403 17. Yount, B., *et al.* Reverse genetics with a full-length infectious cDNA of severe
404 acute respiratory syndrome coronavirus. *Proc Natl Acad Sci U S A* **100**, 12995-
405 13000 (2003).
406